Synthesis, Structures, and Conformation Dynamics of Pyrazolotetrathiepins and Related Compounds Studied by X-ray Crystallography, Dynamic NMR, and Molecular Orbital Calculations†

B. L. Chenard,*‡ D. A. Dixon,* R. L. Harlow, D. C. Roe,* and T. Fukunaga*

Central Research and Development Department, E. I. du Pont de Nemours and Company, Inc., Experimental Station, Wilmington, Delaware 19898

Received January 20, 1987

Pyrazolopentathiepins **1** react with acetone and ammonium sulfide to form pyrazolotetrathiepins **2**, **3**, and **4**. The ketone fragment replaces one of the three inner sulfur atoms in a nearly statistical ratio. The structures of two substituted forms of **2** were ascertained by single-crystal X-ray analysis. Variable-temperature NMR and magnetization transfer experiments show that the relative location of the four sulfur atoms has a pronounced effect on the chair–chair ring inversion barrier, $\Delta G^{\ddagger}$(C–C). For the tetrathiepins containing a trisulfide linkage, **2** and **4**, $\Delta G^{\ddagger}$(C–C) = 18.5 and 17.5 ± 0.1 kcal/mol, respectively, while the isomer **3** possessing two disulfide linkages has $\Delta G^{\ddagger}$(C–C) = 21.2 ± 0.1 kcal/mol. Furthermore, compound **3** exists in solution at room temperature as an equilibrium mixture of chair and twist boat (TB) conformers in a 85:15 ratio, ΔG(C–TB) = 1.16 kcal/mol. The TB–TB inversion barrier, $\Delta G^{\ddagger}$(TB–TB) = 17.7 kcal/mol, is less than the chair–chair inversion barrier by 3.5 kcal/mol. Ab initio calculations on a model tetrathiepin and pentathiepin have been performed with a double ζ basis set augmented by polarization functions on all non-hydrogenic atoms. The geometries of a number of conformers were optimized and force fields were calculated. The theoretical results provide further evidence for the species and energetics involved in the ring inversion process.

Introduction

Organosulfur compounds possessing di-, tri-, and polysulfide linkages have been extensively studied because of their biological activities[1] and the rich chemistry associated with elemental surfur and related reagents.[2,3] Organometallic species with such linkages also have received significant recent interest.[4] However, the isolation of pure samples and unequivocal structural characterization of polysulfides have been plagued by the facile loss of sulfur, rearrangements,[4] and polymerization.[5] This is evident in both acyclic and cyclic polysulfides.[1a] For example, facile equilibration of elemental sulfur to its allotropes at room temperature[6] and some of their structures[7] have been only recently established. Furthermore, information on the structures of various conformers involved in ring inversion and pseudorotation processes of cyclic polysulfides and on their relative energetics is very limited. Theoretical studies of polysulfides are scarce and reliable calculations have been reported only for hydrogen disulfide.[8] Thus, further experimental and theoretical information on the properties of cyclic polysulfur species should greatly facilitate fundamental understanding of not only the chemistry of polysulfur linkages but also the conformational analysis of medium ring systems in general.

We have recently reported the synthesis and characterization of pentathiepins.[1a,b] We have now discovered that pentathiepins readily react with acetone to give the corresponding tetrathiepins and that the latter undergo the complex conformational changes typical of medium ring molecules. In this paper, we describe the results of our studies on the structures, energetics, and conformational dynamics of various tetrathiepin conformers probed by a combination of NMR techniques, X-ray crystallography, and large-scale ab initio molecular orbital calculations. The magnetization transfer technique has been especially useful for complete characterization of the ring inversion process. The ab initio calculations have provided critical insight about the structures and energetics of various conformers involved on the potential energy surface. Furthermore, we have conclusively demonstrated that polarization functions on sulfur are essential to correctly describe the structure and energetics of S–S bonds.

Results

Synthesis, Structure, and Conformation Dynamics. Synthesis of the tetrathiepins is easily effected by the reaction of a pyrazolopentathiepin **1** with acetone in the presence of ammonium sulfide. This ambient temperature transformation takes place within a few hours to afford modest yields of products. In general, we find a nearly

† Contribution No. 3665.

‡ Present address: Pfizer, Central Research, Eastern Point Road, Groton, CT 06340.

(1) For biologically active organopolysulfides see: (a) Chenard, B. L.; Harlow, R. L.; Johnson, A. L.; Vladuchick, S. A. *J. Am. Chem. Soc.* **1985**, *107*, 3871. (b) Chenard, B. L.; Miller, T. J. *J. Org. Chem.* **1984**, *49*, 1221. (c) Chenard, B. L. *J. Org. Chem.* **1984**, *49*, 1224. (d) Saito, T.; Koyama, K.; Natori, S. *Tetrahedron Lett.* **1985**, *26*, 4731. (e) Harpp, D. N.; Smith, R. A. *J. Am. Chem. Soc.* **1982**, *104*, 6045. (f) Anthoni, U.; Christophersen, C.; Jacobsen, N.; Svendsen, A. *Tetrahedron* **1982**, *38*, 2425. (g) Still, I. W. J.; Kutney, G. W. *Tetrahedron Lett.* **1981**, *22*, 1939. (h) Wratten, S. J.; Faulkner, D. J. *J. Org. Chem.* **1976**, *41*, 2465. (i) Kato, A.; Numata, M. *Tetrahedron Lett.* **1972**, 203. (j) Kato, A.; Okutani, T. *Tetrahedron Lett.* **1972**, 2959. (k) Morita, K.; Kobayashi, S. *Chem. Pharm. Bull. Jpn.* **1967**, *15*, 988.

(2) For a summary of the chemistry of sulfur, see: Oae, S. Ed. *Organic Chemistry of Sulfur*; Plenum: New York, 1977; Chapter 2. See also: Chapter 7 for a discussion of the chemistry and biological activity of organic di- and polysulfides.

(3) Kutney, G. W.; Turnbull, K. *Chem. Rev.* **1982**, *82*, 333.

(4) For recent organometallic polysulfur compounds and their chemistry, see: Giolando, D. M.; Rauchfuss, T. B. *J. Am. Chem. Soc.* **1984**, *106*, 6455. Bolinger, C. M.; Rauchfuss, T. B.; Wilson, S. R. *J. Am. Chem. Soc.* **1982**, *104*, 7313; **1981**, *103*, 5620. Bolinger, C. M.; Rauchfuss, T. B. *Inorganic Chem.* **1982**, *21*, 3947. Draganjac, M.; Coucouvanis, D. *J. Am. Chem. Soc.* **1983**, *105*, 139. Muller, A.; Schimanski, J.; Schimanski, U. *Angew. Chem., Int. Ed. Engl.* **1984**, *23*, 159. Weiss, J. *Angew. Chem., Int. Ed. Engl.* **1982**, *21*, 705. Roesky, H. W.; Thomas, M.; Schimkowiak, J.; Jones, P. G.; Pinkert, W.; Sheldrick, G. M. *J. Chem. Soc., Chem. Commun.* **1982**, 895.

(5) For a good example of some of the difficulties in preparing, characterizing, and handling of organopolysulfides, see: Harpp, D. N.; Granata, A. *J. Org. Chem.* **1979**, *44*, 4144.

(6) Tebbe, F. N.; Wasserman, E.; Peet, W. G.; Vatvars, A.; Hayman, A. C. *J. Am. Chem. Soc.* **1982**, *104*, 4971.

(7) Steudel, R. *Top. Curr. Chem.* **1982**, *102*, 149. Steidel, J.; Steudel, R. *J. Chem. Soc., Chem. Commun.* **1982**, 1312. Steudel, R.; Steidel, J.; Pickardt, J.; Schuster, F. *Z. Naturforsch. B* **1980**, *35B*, 1378. Steudel, R.; Reinhardt, R.; Schuster, F. *Angew. Chem., Int. Ed. Engl.* **1977**, *16*, 715.

(8) Dixon, D. A.; Zeroka, D. J.; Wendoloski, J. J.; Wasserman, Z. R. *J. Phys. Chem.* **1985**, *89*, 5334 and references cited therein.

0022-3263/87/1952-2411$01.50/0

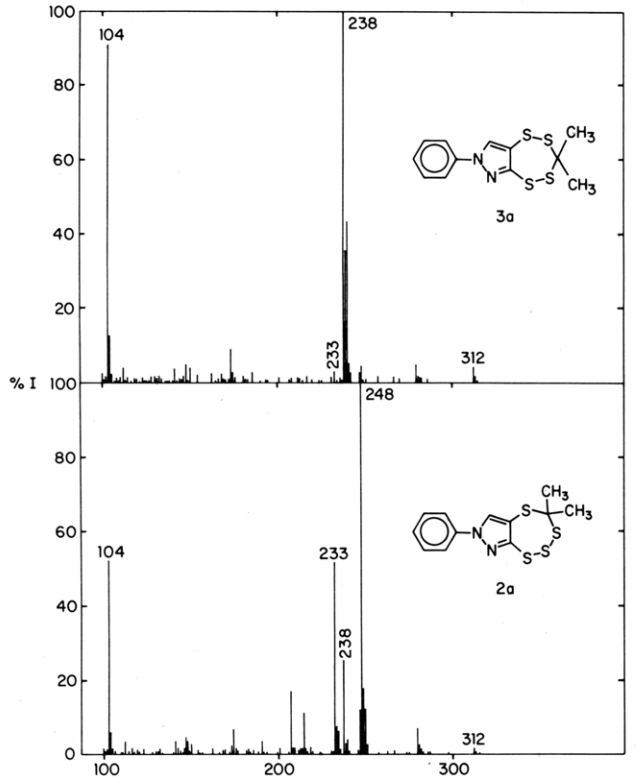

Figure 1. Mass spectral comparison of S-2 and S-3 substitution products.

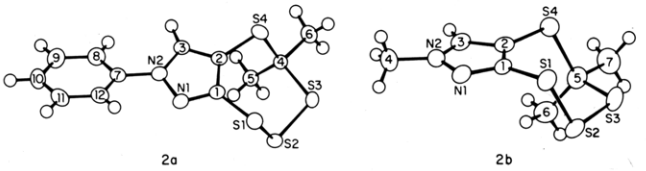

Figure 2. Crystal structures for **2a** and **2b**.

statistical distribution of the ketone fragment in the S2, S3, and S4 sites of the pentathiepin.[9]

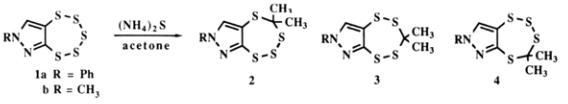

The products were identified by a combination of techniques as described below. The 1,2,4,5-tetrathiepin (**3**) was easily distinguished from the 1,3,4,5- and 1,2,3,5-tetrathiepins (**2** and **4**, respectively) by its mass spectral fragmentation pattern. For example, **3a** has a base peak at m/e 238 due to loss of thioacetone while **2a** and **4a** show a new base peak at m/e 248 due to loss of S_2 (always the major fragmentation for pentathiepins) as well as a smaller fragment at m/e 238 (Figure 1).

Differentiation of the isomers **2a** and **4a** was more difficult. NOE difference spectra (^{1}H NMR) showed a 3.3% enhancement of the pyrazole ring hydrogen of **2a** upon irradiation of the methyl groups attached to the sulfur ring while **4a** showed only a 0.6% enhancement. As this enhancement was indicative but not compelling evidence, we obtained X-ray structures for both **2a** and **2b** (Figure 2) to verify the structural assignment.[10] Apparent in this

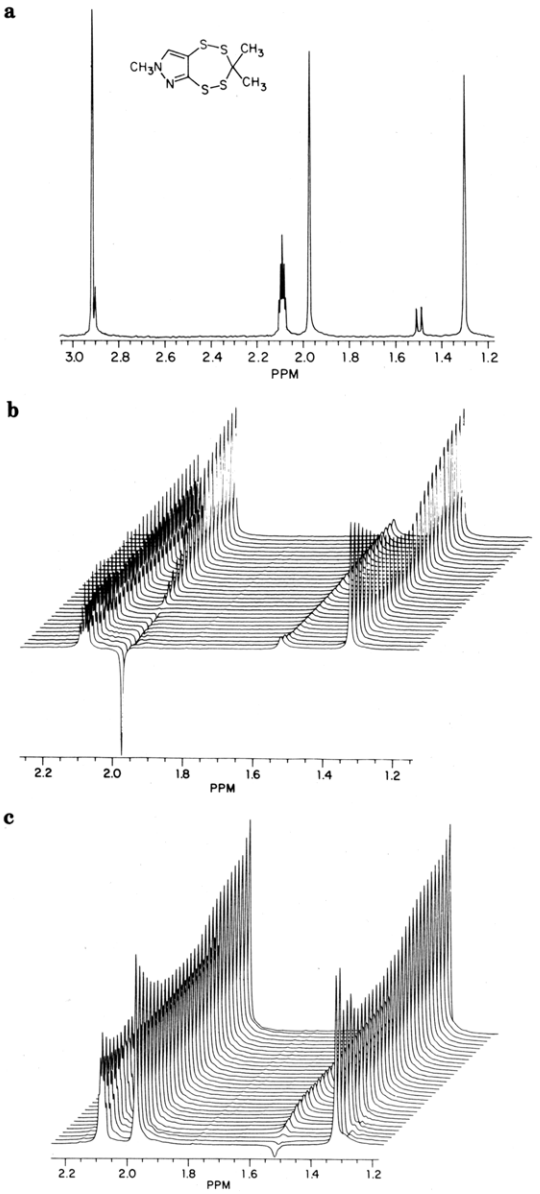

Figure 3. (a) 360-MHz ^{1}H NMR at 30 °C. (b) Inversion transfer—major conformer at 80 °C. (c) Inversion transfer—minor conformer at 80 °C.

figure is the chair conformation of the tetrathiepin ring, which gives rise to nonequivalence of the two methyl groups.

Variable-temperature ^{1}H NMR (360 MHz, toluene-d_8) was used to examine the barrier to ring inversion in the tetrathiepins. In compounds **2** and **4**, coalescense was easily attained between 80 and 100 °C.[11] NMR spectra were simulated over a 50–60 °C temperature range by

(9) This is somewhat surprising since Rauchfuss has reported selective sulfur substitution in a related reaction with Cp_2TiS_5. See: Giolando, D. M.; Rauchfuss, T. B. *Organometallics* **1984**, *3*, 487–489.

(10) Crystal structure information for compound **2a**: $C_{12}H_{12}N_2S_4$, M_r = 312.50, monoclinic, space group $P2_1/n$; at −100 °C, a = 13.386 (2), b = 9.773 (1), and c = 11.551 (1) Å, β = 114.63 (1)°, V = 1373.5 (6) Å, Z = 4, D_i = 1.511 g cm^{-3}; Mo K_2 radiation (λ = 0.71069 Å), μ = 6.47 cm^{-1}. Data were collected on a Syntex P3 diffractometer ($4° < 2\theta < 55°$) by using the ω-scan technique. The refinement of 211 variables (S, N, C with anisotropic thermal parameters, H with isotropic) using 2467 reflections with $I > 2.0\sigma(I)$ converged at R = 0.034 and R_w = 0.031. The magnitude of the largest peak in the final difference Fourier was 0.32 e Å^{-3}. Crystal structure information for compound **2b** (where different from **2a**): $C_7H_{10}N_2S_4$, M_r = 250.43, orthorhombic, space group $Pbca$; at −100 °C, a = 8.293 (1), b = 25.456 (4), and c = 10.736 (2) Å, V = 2266 (1) Å^3, Z = 8, D_c = 1.463 g cm^{-3}, μ = 7.65 cm^{-1}; 158 variables, 1613 reflections, R = 0.041, R_w = 0.033, 0.36 e Å^{-3}. Additional structural information may be found in the supplementary material.

(11) A plot of $\Delta\nu$ vs. temperature showed that the chemical shift of the methyl groups was independent of temperature over a 60° range.

Table I. Activation Energies for Conformational Changes of Tetrathiepins

compd	method	T_c, °C	$\Delta G^{\ddagger}$, kcal/mol	$\Delta H^{\ddagger}$, kcal/mol	$\Delta S^{\ddagger}$, eu
2a	*a*	100	18.5 ± 0.1[d]	16.2 ± 0.9	−6.1 ± 2.6
2b	*a*	100	18.5 ± 0.1[d]	16.1 ± 4.3	−6.4 ± 11.6
4a	*a*	80	17.5 ± 0.1[d]	18.5 ± 2.8	2.8 ± 7.9
3b	*b*		21.2 ± 0.1[e]	22.7 ± 1.1	4.0 ± 2.9
3b	*c*		21.2 ± 0.1[e]	21.8 ± 0.9	1.7 ± 2.4

[a] Dynamic NMR with computer simulation of spectra (line-shape analysis). [b] Combination of magnetization transfer and line-shape analysis. [c] Combination of magnetization transfer, line-shape analysis, and kinetics. [d] Determined at T_c. [e] Determined at 100 °C.

using the standard DNMR3 program[12] to obtain exchange rates that yielded the activation parameters in Table I.

Compound **3** shows a much more pronounced difference in chemical shift of the methyl groups (~0.6 ppm compared to 0.1 ppm for **2** and **4**). For **3b**, coalescence of the methyl signals was not observed even at 140 °C (*o*-xylene-d_{10}), and complete band-shape analysis was therefore restricted to the initial line-broadening changes from 110 to 140 °C. In order to extend the temperature range of the line-shape analysis, magnetization transfer experiments[13] were also carried out.

The methyl region of the ^{1}H NMR spectrum of **3b** is illustrated in Figure 3a (30 °C); note the additional small pair of singlets around 1.5 ppm. Selective inversion of the methyl resonance at 1.97 ppm (Figure 3b, 80 °C) results in the characteristic decay and recovery of the other methyl signal (1.30 ppm) that is indicative of exchange between these resonances. However, the minor pair of singlets (coalesced at 80 °C) also shows the same decay and recovery pattern. Selective inversion of this minor component (Figure 3c) clearly demonstrates exchange into both methyl groups of the major component.

Based on the X-ray data reported here, as well as that described elsewhere for benzotetrathiepins[14] and pentathiepins,[1a] we assign the chair conformer as the dominant species of **3b** in solution. This assignment is supported by the observation of the major conformer as the only species present (from −80 to −30 °C) when crystalline **3b** was dissolved in toluene-d_8 at dry ice temperature and transferred to the spectrometer without warming. Equilibration with the minor isomer proceeds at a rate conveniently monitored by conventional ^{1}H NMR kinetics at −10 °C ($k = 1.35 \times 10^{-5}$ s^{-1}). This minor species is assigned as the twist-boat conformer on the basis of related assignments in the 1,2,4,5-tetrathiin series[15] and the similar chemical shifts of the *gem*-dimethyl group. Whereas the methyl groups in the twist-boat form are positioned in nearly identical chemical environments and are expected to show similar chemical shifts, the two methyls would be in significantly different magnetic environments in the boat form, another possible structure for the minor conformer.

Line-shape changes associated with interconversion of the minor methyl groups at 60 °C (near coalescence) and above lead to an estimate for the twist-boat interconversion

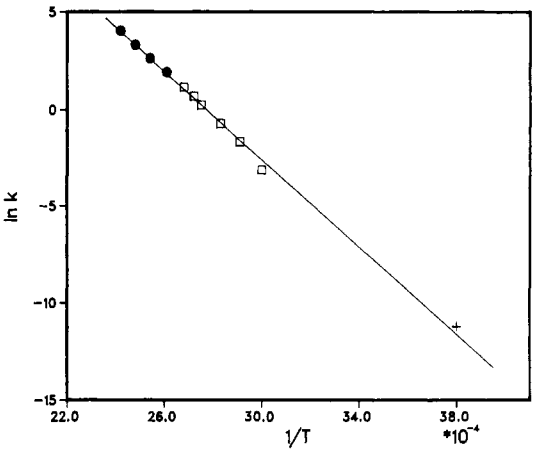

Figure 4. NMR data used in determining $\Delta H^{\ddagger}$ and $\Delta S^{\ddagger}$ for **3b**. The open squares are magnetization transfer data, the filled circles are from line-shape analysis, and the cross is from a kinetics measurement.

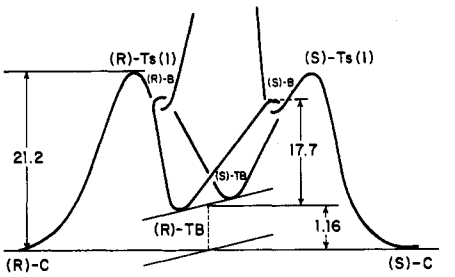

Figure 5. Section of potential energy hypersurface for conformational changes of 1,2,4,5-tetrathiepin **3b**. The numbers indicate the experimentally determined energies (ΔG and $\Delta G^{\ddagger}$ in kcal/mol. See text and Figure 6 for more detailed description of the energy surface in the region of the boat conformer.

barrier $\Delta G^{\ddagger}$(60 °C) = 17.7 kcal/mol. Magnetization transfer data from 60 to 100 °C were fitted to an exchange model, which involved chair–chair interconversion by way of the twist-boat intermediate. The initial line-broadening changes from 110 to 140 °C were analyzed as a nonmutual exchange between the methyls of the chair conformer and the rapidly interconverting methyls of the twist-boat; rates for the latter process were estimated from 110 to 140 °C according to the activation barrier determined above. Rate constants from both methods were combined (Figure 4) to give the activation parameters listed in Table I (method b). Extrapolation of these results to −10 °C leads to an estimated rate for chair to twist-boat interconversion of 0.54×10^{-5} s^{-1}; thus the observed rate of 1.35×10^{-5} s^{-1} (see Figure 4) is easily within the error limits obtained by propagating the errors in the activation parameters. If the observed rate constant (at −10 °C) is included in the activation analysis, $\Delta H^{\ddagger}$ = 21.8 ± 0.9 kcal/mol and $\Delta S^{\ddagger}$ = 1.7 ± 2.4 eu (Table I, method c).

From the equilibrium constant measured by integration of the ^{1}H NMR signals due to each conformer, an energy difference ΔG = 1.16 kcal/mol between the chair and twist-boat ground states is calculated. Since this energy difference was found to be only very slightly dependent on temperature within the range of measurements, ΔS is small and $\Delta G \sim \Delta H$. These features are summarized along with the results of the activation analysis by the energy diagram illustrated in Figure 5.

It is interesting to note that the chair to chair interconversion is 3.5 kcal/mol ($\Delta\Delta G^{\ddagger}$ at 60 °C) more difficult than the twist-boat interconversion. This observation is consistent with the notion that the two processes proceed through different transition states. Examination of

(12) Spectra were calculated by using DNMR3. Kleier, D. A.; Binsch, G. "DNMR3: A Computer Program for the Calculation of Complex Exchange-Broadened NMR Spectra. Modified Version for Spin Systems Exhibiting Magnetic Equivalence of Symmetry," Program 165, QCPE, Indiana University, 1970.

(13) Forsen, S.; Hoffman, R. A. *J. Chem. Phys.* **1963**, *39*, 2892–2901; **1964**, *40*, 1189–1196.

(14) Feher, F.; Malcharek, F.; Glinka, K. *Angew. Chem., Int. Ed. Engl.* **1971**, *10*, 331. Feher, F.; Engelen, B. *Z. Naturforsch. B* **1979**, *34*, 426.

(15) Bushweller, C. H. *J. Am. Chem. Soc.* **1967**, *89*, 5978–5979.

Table II. Calculated and Experimental Geometric Parameters[a] for Conformers of 5, 7, and 8

parameter	5-C	7[b]	8[b]	5-B	5-TB	5-Ts(1)
$r(C_1{=}C_{1'})$	1.326	1.408	1.399	1.331	1.326	1.326
$r(C_1{-}H)$	1.076			1.076	1.078	1.075
$r(C_1{-}S_1)$	1.778	1.760	1.767	1.776	1.775	1.775
$r(S_1{-}S_2)$	2.061	2.032	2.028	2.102	2.053	2.081
$r(S_2{-}C_2)$	1.815	1.801	1.817	1.811	1.816	1.845
$r(C_2{-}H_2)$	1.078			1.084	1.082	1.068
$r(C_2{-}H_3)$	1.082			1.076	(1.082)	1.117
$\theta(H_1C_1C_{1'})$	118.9			119.7	117.5	120.0
$\theta(H_1C_1S_1)$	115.3			117.3	110.9	118.1
$\theta(C_{1'}C_1S_1)$	125.8	122.2	123.0	123.1	131.6	121.9
$\theta(C_1S_1S_2)$	103.2	104.8	105.1	102.4	104.8	104.0
$\theta(S_1S_2C_2)$	102.9	103.6	104.1	104.7	103.2	115.5
$\theta(S_2C_2S_{2'})$	117.2	115.2	112.8	122.6	116.3	126.5
$\theta(S_2C_2H_2)$	109.8			104.0	111.0	106.2
$\theta(S_2C_2H_3)$	105.3			108.9	104.5	105.2
$\theta(H_2C_2H_3)$	109.0			107.3	108.7	106.0
$\tau(S_1C_{1'}C_1S_1)$	0.0	2.9		0.0	0.8	0.0
$\tau(C_{1'}C_1S_1S_2)$	74.6	76.2	74.7	80.2	36.9	82.6
$\tau(C_1S_1S_2C_2)$	82.2	86.7	86.8	30.0	88.3	57.3
$\tau(S_1S_2C_2S_{2'})$	76.8	74.3	75.9	64.4	44.7	0.0

[a] Bond distances in Å. Bond angles in degrees. [b] Reference 14.

Scheme I. Ring Inversion and Pseudorotation Process of 1,2,4,5-Tetrathiepin 3b

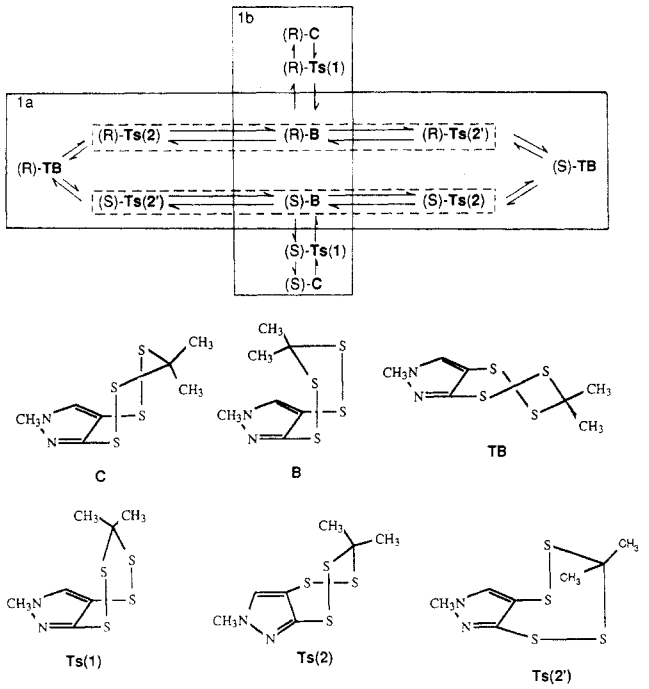

Dreiding models shows that the flexible twist-boat enantiomer, (*R*)- or (*S*)-TB, racemizes through a conrotatory (about the two S–S bonds) pseudorotation pathway via a boat conformer, (*R*)- or (*S*)-B. There are two degenerate diastereomeric pathways for this process involving either clockwise or counterclockwise conrotation. The boat form may either be the transition state or an intermediate along the reaction coordinate. If the latter is the case, the transition state may resemble one of the diastereomeric pairs, (*R*)/(*S*)-Ts(2) or (*R*)/(*S*)-Ts(2′), which have the five contiguous atoms, SCCSS, in a plane. Scheme Ia summarizes the pseudorotation process, where possible transition state structures are blocked by a dotted line. Models also show that the chair–chair interconversion, (*R*)-C ↔ (*S*)-C, proceeds first by way of a disrotatory motion about the two S–S bonds to bring the sp^3 carbon in the plane of the sulfur atoms. Continuation of the motion along this reaction coordinate connects the chair to the corresponding enantiomeric boat conformer (Scheme Ib). Racemization

Table III. Calculated and Experimental Geometric Parameters[a] for Conformers of 6 and 9

parameter	6-C	9[b]	6-B	6-TB	6-Ts(1)
$r(C_1{=}C_{1'})$	1.327	1.355	1.330	1.326	1.327
$r(C_1{-}H)$	1.076		1.075	1.077	1.076
$r(C_1{-}S_1)$	1.782	1.762	1.772	1.777	1.781
$r(S_1{-}S_2)$	2.067	2.053	2.128	2.051	2.052
$r(S_2{-}S_3)$	2.067	2.051	2.048	2.077	2.130
$\theta(HC_1S_1)$	115.1		116.7	110.4	117.9
$\theta(HC_1C_{1'})$	118.0		118.7	117.3	120.7
$\theta(C_{1'}C_1S_1)$	126.8	126.8	124.6	132.3	121.4
$\theta(C_1S_1S_2)$	103.0	104.6	103.0	103.7	103.1
$\theta(S_1S_2S_3)$	104.3	104.4	105.1	105.7	113.2
$\theta(S_2S_3S_{2'})$	103.9	102.8	108.5	102.4	119.4
$\tau(S_1C_1C_{1'}S_{1'})$	0.0	−1.2	0.0	1.7	0.0
$\tau(C_1S_1S_2S_3)$	87.9	88.2	21.3	93.8	56.2
$\tau(S_1S_2S_3S_{2'})$	76.1	77.4	68.6	46.2	6.0
$\tau(C_{1'}C_1S_1S_2)$	76.2		80.5	39.6	90.6

[a] Bond distances in Å. Bond angles in degrees. [b] Reference 16.

within the boat framework discussed above followed by a reverse of the initial disrotatory process completes the chair–chair interconversion. The transition state for the disrotatory inversion process may be approximated by the structure that has all of the four sulfur atoms and the sp^3 carbon atom in a plane, (*R*)/(*S*)-Ts(1). The relationship between the two processes along the two different coordinates and the species involved in the processes are summarized in Scheme I and depicted together with the experimentally determined energies in Figure 5.

Theoretical Studies. In order to provide more information about various structural features on the potential energy hypersurface, we performed ab initio molecular orbital calculations on the parent tetra- and pentathiepins, **5** and **6**, respectively. The ground-state chair structure (C)

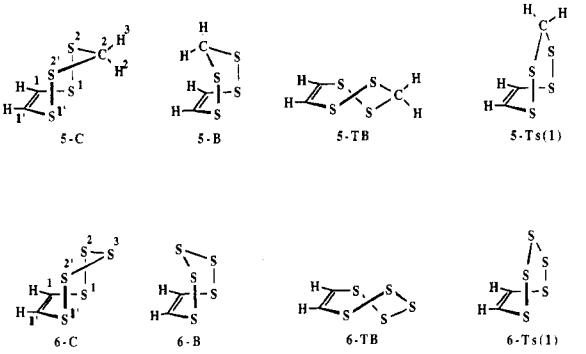

with C_s symmetry, the C_s boat conformation (B), the C_2 twist-boat conformation (TB), and the C_s structure for transition state, Ts(1), were calculated. The structural parameters for the conformations of **5** are given in Table II and those for **6** in Table III where the chair structures are compared to experimental crystal structures, **7**, **8** and **9**.

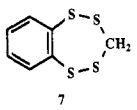

7

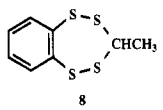

8

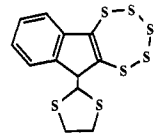

9

We compare **5**-C to 1,2,4,5-tetrathiepins **7** and **8**, the only two available crystal structures.[14] The major difference is the length of the C=C bond that is an olefinic double bond in **5** and aromatic in **7** and **8**. This has a small effect on the S–S bond lengths which are calculated to be 0.03 Å longer than the experimental values. With this basis set (see Experimental Section) the S–S bond in H_2S_2 is calculated to be 0.01 Å too long. Even with the correction factor our calculated value for r(S–S) is approximately 0.02 Å too long and it probably reflects the difference in the C=C bond lengths. The two calculated C–S bond distances, $r(C_1–S_1)$ and $r(C_2–S_2)$, are in excellent agreement with the experimental values. The $C_1–S_1$ bond length is shorter than the $C_2–S_2$ bond length, consistent with C_1 being a trigonal sp^2 carbon and C_2 being a tetrahedral sp^3 carbon. The calculated $C_{1'}C_1S_1$ and $S_2CS_{2'}$ bond angles are slightly larger than the experimental values, again reflecting the shorter C=C bond. The bond angles at sulfur are in excellent agreement and are about 4° larger than the HSS bond angle in H_2S_2. The torsion angles about the various bonds are in good agreement. For the torsion about the S–S bond, the experimental value is 4.5° larger than the calculated value but both are close to the optimum torsion angle of 90° found in H_2S_2, suggesting that there is little torsional strain in this conformation.

Many of the geometric parameters for the twist-boat structure **5**-TB are very similar to those of the optimum chair form **5**-C. The $C_{1'}C_1S_1$ bond angles opens up and the $H_1C_1S_1$ angles decreases in **5**-TB as compared to **5**-C. The only significant changes are found for the two torsion angles $\tau(C_{1'}C_1S_1S_2)$ and $\tau(S_1S_2C_2S_{2'})$, which are both decreased by about 50%. However the torsion angle about the S–S bond in **5**-TB actually is closer to the optimum value of 90°.

In **5**-B, there are larger changes in the structure due to the unfavorable torsion angle about the S–S bond of 30°. This leads to an increase in the S–S bond length consistent with the increase 0.051 Å observed in the cis structure for H_2S_2. Furthermore the C=C bond stretches slightly and the $S_2C_2S_{2'}$ angle opens up by about 5°.

For **5**-Ts(1), the largest variations are found in $\theta(S_1S_2C_2)$ and $\theta(S_2C_2S_{2'})$ which open up by 10° and 4°, respectively, relative to the boat structure. The torsion angle about the S–S bond is near 60°; the parameters in the double-bond region are essentially the same as those for the boat; the S–S bond length is between the boat and chair values; and the $S_2–C_2$ bond length increases by about 0.03 Å relative to the other conformers.

For the pentathiepin, excellent agreement is found between the calculated structure **6**-C and the crystal structure of **9**,[16] which has the shortest C=C ring bond known for pentathiepins. Correcting the calculated S–S bond lengths by 0.01 Å gives excellent agreement with the experimental values. The agreement of the chair structures between theory and experiment suggests that our method can provide a good description of the geometric parameters for this class of molecules. An important feature to note is that all of the torsion angles about the S–S bonds in the chair form for **6**-C are near 90°, the optimum value for H_2S_2.

Table IV. Relative Energetics (in kcal/mol) for Conformers of 5 and 6

structure	ΔE(SCF)	ΔE(MP-2)	cmpd	$\Delta G^{\ddagger}$(expt)
5-C	0.0	0.0	**3**-C	0.0
5-B	14.5	13.5	**3**-B	18.9[a]
5-TB	0.36	−0.41	**3**-TB	1.16[a]
5-Ts(1)	20.8	21.3	**3**-Ts(1)	21.2[a,b]
6-C	0.0	0.0	**10**-C	0.0
6-B	14.9	13.1		
6-TB	5.2	4.1	**10**-TB	*c*, *e*
6-Ts(1)	28.6	29.2	**10**-Ts	19.3[c,d]

[a] This work on **3**. [b] $\Delta H^{\ddagger}$ = 21.8 kcal/mol. [c] Reference 17 for **10**. [d] Structure not defined by experiment. See text. [e] Not observed.

The structural parameters for the twist-boat conformer **6**-TB change slightly from those of **6**-C. The $S_2–S_3$ bond distance increases by 0.01 Å while the $S_1–S_2$ bond distance decreases by 0.016 Å in **6**-TB. Following the behavior of **5**-TB, the $C_{1'}C_1S_1$ bond angle opens up in **6**-TB as compared to **6**-C. The major change in **6**-TB as compared to **6**-C is the large decrease in the torsion angles about the $S_2–S_3$ and $C_1–S_1$ bonds. The 46° torsion angle about the $S_2–S_3$ bond in **6**-TB is clearly far from the optimum value of 90° for an S–S bond.

In **6**-B, the torsion angle about the $S_1–S_2$ bond is approaching 0° (21.3°). (There are, of course, two such torsion angles.) This leads to a significant increase of 0.061 Å in the $S_1–S_2$ bond length (see above). The $S_2–S_3$ bond that has a torsion angle closer to 90° (68.6°) actually shows a decrease in bond length of 0.019 Å. This type of behavior is expected on the basis of the structure of S_7.[7] The other major difference is the increase of 4.6° in the bond angle at the unique sulfur, S_3.

For **6**-Ts(1), both HC_1S_1 and $HC_1C_{1'}$ bond angles open up while the $C_{1'}C_1S$ angle decreases. In spite of these angle changes, the bond lengths involving the carbons remain essentially unchanged. The $S_1–S_2$ bond length decreases relative to **6**-C and is similar to that in **6**-TB. Due to the high energy torsion angles involving the $S_2–S_3$ and $S_{2'}–S_3$ bonds, the $S_2–S_3$ and $S_{2'}–S_3$ bond lengths increase significantly to 2.130 Å. The approximate planarity of the sulfur atoms also leads to significant increase in the bond angles at S_2 and S_3 by 9° and 16°, respectively, relative to **6**-C. Besides the torsion angles about the $S_2–S_3$ and $S_{2'}–S_3$ bonds being far from optimal, there is also some deviation from the optimal value about the $S_1–S_2$ and $S_{1'}–S_{2'}$ bonds.

In Table IV we present the relative energies of the conformers calculated at the SCF and MP-2 levels, together with the experimental values for **3** and the results of Raban and Chenard[17] on **10**.

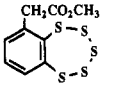

10

In Table V, we present the calculated vibrational frequencies for the various structures of **5**. The vibrational

(16) Korp, J. D.; Bernal, I.; Watkins, S. F.; Fronczek, F. R. *J. Heterocycl. Chem.* **1982**, *19*, 459.

(17) Raban, M.; Chenard, B. L. *J. Org. Chem.*, in press.

Table V. Calculated Vibrational Frequencies (cm^{-1}) and Infrared Intensities (km/mol) for Tetrathiepin 5

	5-C[a]		5-B[a]		5-Ts(1)[a]		5-TB[b]	
sym	ν	I	ν	I	ν	I	ν	I
A′	3405	23.2	3403	19.3	3428	11.0	3388	13.0
	3368	2.6	3363	6.4	3415	19.8	3266	22.4
	3275	12.0	3269	4.5	2966	18.9	1776	17.3
	1769	9.8	1739	9.3	1761	8.8	1595	0.6
	1563	5.1	1583	7.4	1653	3.5	1341	0.0
	1317	1.0	1296	2.4	1286	1.7	1268	0.0
	922	11.6	912	22.8	931	0.3	1066	0.6
	824	68.8	834	67.0	830	76.2	722	0.6
	731	1.4	749	3.0	754	3.0	689	1.8
	710	3.6	703	2.5	688	0.2	562	0.0
	542	0.8	511	0.6	491	0.7	482	0.3
	385	1.5	411	0.2	418	0.4	402	0.8
	286	0.7	271	0.1	247	0.6	262	0.1
	250	0.3	255	2.6	211	0.6	180	0.0
	151	3.4	189	0.3	173i[c]	6.8		
A″	3383	0.4	3381	0.6	3393	0.2	3367	0.6
	1458	4.6	1450	9.4	1442	2.4	3335	2.5
	1385	15.9	1409	22.2	1432	6.6	1466	8.9
	1302	3.0	1313	2.0	1244	0.3	1384	6.4
	1084	8.2	1079	5.0	1071	7.1	942	3.9
	902	1.2	903	0.4	903	0.1	878	17.7
	834	16.0	850	24.1	855	0.0	841	9.6
	602	3.5	588	0.5	591	0.8	760	73.2
	563	0.4	555	0.1	543	0.2	663	3.4
	461	1.0	448	0.4	447	1.5	550	2.2
	192	0.1	199	0.2	178	0.1	252	1.9
	150	3.2	43i[c]	0.3	80	2.1	203	3.1
							109	6.0

[a] C_s symmetry. [b] C_2 symmetry. A′ = A_1, A″ = A_2. [c] Imaginary frequency.

Table VI. Calculated Vibrational Frequencies (cm^{-1}) and Infrared Intensities (km/mol) for Pentathiepin 6

	6-C[a]		6-B[a]		6-Ts(1)[a]		6-TB[b]	
sym	ν	I	ν	I	ν	I	ν	I
A′	3404	19.9	3411	15.6	3412	13.3	3383	8.8
	1767	10.5	1742	7.7	1754	5.7	1774	18.2
	1328	1.3	1316	2.4	1283	1.4	1350	0.0
	827	68.4	838	68.3	840	76.1	1071	0.5
	719	2.4	744	3.4	749	2.0	683	2.3
	538	4.8	555	1.4	576	0.1	559	1.0
	520	0.9	484	1.5	421	0.4	520	0.5
	335	2.6	348	0.5	349	0.5	475	0.0
	269	1.4	247	1.4	230	0.1	331	3.0
	222	0.1	211	2.2	205	1.1	249	0.2
	138	0.7	171	0.3	199i[c]	1.1	175	0.0
A″	3382	0.4	3389	0.7	3390	0.4	3363	1.1
	1455	1.1	1450	0.8	1437	0.2	1465	2.9
	1087	7.2	1068	8.6	1068	2.7	875	17.0
	895	1.1	906	0.3	903	0.1	764	73.4
	601	3.6	581	2.6	590	2.2	664	4.0
	543	1.0	555	3.3	560	5.2	544	1.0
	528	0.0	512	0.4	519	6.1	538	5.2
	459	0.9	429	0.5	452	4.9	228	5.2
	188	0.0	189	0.1	167	0.1	195	2.0
	159	1.8	59i[c]	0.6	83	2.8	82	1.2

[a] C_s symmetry. [b] C_2 symmetry. A′ = A_1, A″ = A_2. [c] Imaginary frequency.

frequencies show that **5**-C and **5**-TB are minima on the potential energy surface since there are no imaginary frequencies. Both **5**-B and **5**-Ts(1) have one imaginary frequency and are thus transition states. The frequencies are of different symmetry types being of A′ symmetry (symmetric) for **5**-Ts(1) and of A″ symmetry (asymmetric) for **5**-B. Thus the two motions are orthogonal to each other. The imaginary frequency motion for **5**-Ts(1) is a rock of the CH_2 group in the mirror plane and corresponds to the motion inverting the chair to the boat. The imaginary frequency motion of **5**-B corresponds to twisting of the ring, which is the motion connecting the boat to the twist-boat structure. The frequencies should all be scaled by a scale factor of ~0.9 to account for correlation corrections and anharmonicity effects. For example, the C=C stretch calculated in the mid 1700 cm^{-1} range gives scaled values near 1600 cm^{-1} in good agreement with that of other olefins. The size of the imaginary frequencies is quite different for the two transition states; **5**-Ts(1) with a higher frequency of 173i cm^{-1} is a tighter transition state as compared to **5**-B with the low value of 43i cm^{-1} which is a floppier transition state.

The vibrational frequencies for pentathiepin **6** are given in Table VI. Again **6**-C and **6**-TB are minima on the potential energy surface with no imaginary frequencies while **6**-B and **6**-Ts(1) are transition states each charac-

terized by one imaginary frequency. The motions for the imaginary frequencies for 6-B and 6-Ts(1) are orthogonal as found for 5-B and 5-Ts(1) and can be described in the same manner. For 6-Ts(1) the imaginary frequency corresponds to motion of S_3 in the mirror plane while for 6-B the motion corresponds to twisting the ring and breaking the mirror plane symmetry.

Discussion

The barriers to ring inversion of **2**, **3**, and **4** in Table I may be compared with those for benzocycloheptenes and related thiepins. Benzocycloheptene **11** is reported to invert with a barrier of 10.9 kcal/mol,[18,19a] and a *gem*-dimethyl group in **12** and **13** raises the barrier by as much as 0.9 kcal/mol to 11.8 and 11.4 kcal/mol,[19] respectively.

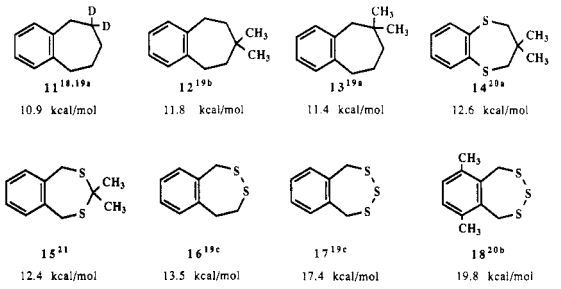

Benzodithiepins **14**[20a] and **15**[21] with two isolated sulfur atoms and a *gem*-dimethyl group exhibit inversion barriers of 12.6 and 12.4 kcal/mol, so that one may conclude that an isolated sulfur atom raises the barrier by 0.3–0.4 kcal/mol. By contrast, a disulfide linkage increases the barrier by 2.6 kcal/mol (**11** vs. **16**) and a trisulfide linkage by 6.5 kcal/mol (**11** vs. **17**). The inversion barriers for tetrathiepins **2** and **4** may be estimated by using **11** as the base and adding the increment due to a trisulfide linkage, a *gem*-dimethyl group, and another isolated sulfur. The estimated value of 18.7 kcal/mol is in good agreement with those determined for **2** and **4**. However, because the trisulfide contribution dominates the correction term, the barrier for trithiepin **17** is very similar not only to the above estimate but also to the observed barrier for **2** and **4**. Similar inversion barriers also have been noted for benzopentathiepin **10** and trithiepin **18**.[17] These relationships may be regarded as being indicative of a resemblance of the ground- and transition-state structures among these compounds. However, a similar additivity breaks down for tetrathiepin **3**, where the barrier is estimated at least 4 kcal/mol less than the observed value. Currently, information on conformation dynamics is very limited for medium ring systems.[22a] Although the chair conformation is generally assumed to be the minimum energy structure, little is known of the relative energies of a variety of conformers and transition-state structures involved in such conformational equilibria.

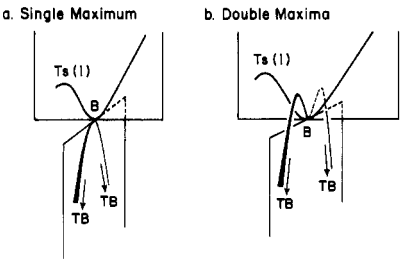

Figure 6. Energy profiles around the boat conformer.

Tetrathiepins. For tetrathiepin **3b**, we have established the presence of two interconverting conformers and two transition states by NMR experiments. Based on the low temperature NMR data and X-ray structures of related compounds, we have assigned the chair structure, **3**-C, to the major species in the equilibrium. Although the assignment of the twist-boat conformer **3**-TB to the minor isomer also appears convincing (vida supra), earlier workers have made assignments of a boat form to the minor component of certain benzocycloheptene derivatives.[19,22b] Our ab initio molecular orbital studies of the parent 1,2,4,5-tetrathiepin (**5**) provide relevant new information on the species and energy surface involved in the conformation dynamics of **3b**.

As shown in Table IV, the twist-boat form (**5**-TB) of the parent tetrathiepin **5** is 0.36 kcal/mol above the chair form (**5**-C) at the SCF level. Although the MP-2 corrected value places **5**-TB 0.41 kcal/mol below **5**-C, we regard the values to be in good agreement with the energy difference of 1.16 kcal/mol found between the major and minor conformers of **3b**, considering the structural differences between the two systems especially in the C=C bond length. By contrast, the boat form **5**-B is calculated to be 13–15 kcal/mol less stable than the chair **5**-C. We regard this as confirmatory evidence for assigning the twist-boat **3**-TB, not the boat structure **3**-B, to the minor conformer in solution of **3b**. Also, good agreement is found between the activation energy determined for the chair–chair interconversion of **3b** and the energy of **5**-Ts(1) calculated relative to **5**-C. This result together with the finding that **5**-Ts(1) has one imaginary frequency for methylene rock is consistent with the assignment of **3**-Ts(1) to the transition state for the **3**-C inversion process.

The transition state for the TB–TB interconversion on the energy surface of **5** turns out to be the boat conformer **5**-B. Our search for structures akin to Ts(2) on the energy surface of **5** by the sigma optimization technique has always led to a structure that is lower in energy than **5**-B; thus **5**-Ts(2) cannot serve as the transition state for the process. We find that the boat conformer, **5**-B, has one imaginary frequency along the pseudorotation coordinate, while it has a real frequency for the methylene rock. The two reaction coordinates are mutually orthogonal at the boat form **5**-B that is the transition state for the TB–TB interconversion but a minimum along the disrotatory pathway toward **5**-C via **5**-Ts(1). The boat form region of the energy surface depicted in a general form in Figure 5 can now be described in more detail. Although the surface shown in Figure 6a with a single maximum along the TB–TB conversion pathway appears to be a special case of the double maxima surface shown in Figure 6b, the theoretical results are consistent only with the single maximum surface. It should be noted that after the chair form passes Ts(1), the inversion motion (methylene rock) couples with the orthogonal pseudorotation motion that twists the methylene group and the molecule can fall directly into the twist-boat form without accessing the boat form.

(18) Sutherland, I. O. in *Advances in Magnetic Resonance*; Waugh, J. S., Ed.; Academic Press: New York, 1967; p 129. For nonfused systems, the value is much lower.

(19) (a) Kabuss, S.; Friebolin, H.; Schmid, H. G. *Tetrahedron Lett.* **1965**, 469. (b) Kabuss, S.; Schmid, H. G.; Friebolin, H.; Faisst, W. *Org. Magn. Reson.* **1970**, *2*, 19. (c) Kabuss, S.; Luttringhaus, A.; Friebolin, H.; Schmid, H. G.; Mecke, R. *Tetrahedron Lett.* **1966**, 719.

(20) (a) Von Bredow, K.; Friebolin, H.; Kabuss, S. *Org. Magn. Reson.* **1970**, *2*, 43. (b) Von Bredow, K.; Jaeschke, A.; Schmid, H. G.; Friebolin, H.; Kabuss, S. *Org. Magn. Reson.* **1970**, *2*, 543.

(21) Schmid, H. G.; Friebolin, H.; Kabuss, S.; Mecke, R. *Spectrochim. Acta* **1966**, *22*, 623.

(22) (a) See, for example: Bocian, D. F.; Strauss, H. L. *J. Am. Chem. Soc.* **1977**, *99*, 2876. (b) Grunwald, E.; Price, E. *J. Am. Chem. Soc.* **1965**, *87*, 3139.

We believe that the energy surface derived for **5** that includes the boat conformer as the transition state for the TB–TB conversion is consistent with the experimental data obtained for **3b**. Although the activation energy of 17.7 kcal/mol observed for the TB–TB interconversion of **3b** is 4 kcal/mol greater than the calculated energy difference of 13.9 kcal/mol between **5**-B and **5**-TB, the difference of this magnitude may be exactly what is expected of the *gem*-dimethyl group in **3**. The methyl groups would sterically destabilize the boat form **3**-B relative to the model system **5**-B but would only slightly perturb the energies of other conformers such as the chair, twist-boat, and Ts(1). Thus, the relative energies between various conformers are expected to be comparable for the two systems, **3** and **5**, unless the boat form is involved. Furthermore, since the boat form **5**-B is calculated to be higher in energy than **5**-Ts(2) and it is a maximum along the TB–TB interconversion pathway, **3**-B with a *gem*-dimethyl group is certainly expected to be less stable than **3**-Ts(2) and the single maximum energy surface depicted in Figure 6a should prevail.

Pentathiepins. For pentathiepin **6**, the energy difference between the chair and twist-boat form (**6**-C and **6**-TB) is calculated to be significantly larger than that for tetrathiepin **5**. The difference of 4–5 kcal/mol (see Table IV) is large enough so that the twist-boat **6**-TB will not be observed by NMR. In fact, only one conformer can be detected in solutions of pentathiepin **10**.[17] Furthermore, since the boat forms **5**-B and **6**-B are equally destabilized relative to the corresponding chair form, the energy difference between TB and B is also about 4–5 kcal/mol larger for **5** than for **6**; thus, the pentathiepin should pseudorotate more readily than the tetrathiepin. The expected transition state **6**-Ts(1) for ring inversion is calculated to have one imaginary frequency, like **5**-Ts(1), along the direction appropriate for ring inversion and is located 28.6 kcal/mol (SCF), 29.2 kcal/mol (MP-2), above the chair form **6**-C. This energy difference is more than 7 kcal/mol greater than the corresponding energy difference for the pentathiepin **5** as predicted also on the basis of additional S–S torsion strain in **6** (vida infra). These results suggest that the relatively small activation energy of 19.3 kcal/mol reported for ring inversion of **10**[17] may not be due to an unassisted unimolecular process.

Torsion Potentials. The dominant structural factor leading to the various energy differences is the torsion potential about the S–S bond. As described in the Experimental Section, reliable theoretical descriptions about the conformational properties and energetics of the S–S bonds can be obtained only with a basis set which is at least a split valence basis set with polarization function.[23] Our calculations show that the torsion angles about the S–S bonds in **5**-C and **5**-TB are nearly optimal, and to first order they should be isoenergetic (and indeed they are). This result also implies that varying the torsion angle about a C–S bond does not significantly alter the energy. For the boat form **5**-B, the torsion angles about the S–S bonds are clearly not optimim. Earlier, one of us reported that the cis form of H_2S_2 is calculated to be 8.2 kcal/mol less stable than the optimum structure at the SCF-CISD level, by 7.5 kcal/mol if zero-point energy effects are included.[8] At the S–S torsion angle of 30° calculated for **5**-B, there should be an increase of 5.5 kcal/mol over that for the optimum structure.[24] Since there are two such S–S bonds in **5**-B, the major part of the energy difference of 14.5 kcal/mol between **5**-C and **5**-B is attributed to the torsion strain about the S–S bonds. Opening up the bond angle at the methylene carbon also contributes to an increase in the angle strain. For structure **5**-Ts(1) with five of the seven ring atoms in a plane, angle strain appears to become the major factor. The two S–S torsion angles deviate only by 30° from the optimum value leading to destabilization of 2.8 kcal/mol.[24] By contrast, the SCS and $S_1S_2C_2$ angles open up by 9° and 12°, respectively, from the corresponding optimum value in the chair structure and this angle strain probably accounts for most of the strain.

In pentathiepin **6** there are more S–S bonds and the S–S torsion can play a larger role in determining relative energies of its conformers. The torsion angle of 46.2° about the S_2–S_3 bond in **6**-TB would lead to an increase of 3.1 kcal/mol per S–S bond.[24] Thus, we estimate that **6**-TB would be 6.2 kcal/mol less stable than **6**-C. The calculated energy difference of 4.1 kcal/mol indicates that there is some other relaxation in **6**-TB that compensates for the torsion strain. Since substitution of the central sulfur atom in **6** by a methylene group to give **5** eliminates this torsion strain, consideration of torsion strain alone leads to a correct prediction that the twist-boat form could be seen in the tetra- but not in pentathiepins. The boat form **6**-B has two torsion angles near 20° and two near 70°, which contribute to destabilization of 6.7 and 0.5 kcal/mol per S–S bond, respectively.[24] This leads to an estimate of a 14.4 kcal/mol total destabilization for **6**-B relative to **6**-C, that is in good agreement with the calculated value of 14.9 kcal/mol. In structure **6**-Ts(1) there are two high energy torsions involving the bonds to S_3 and these each contribute 7.9 kcal/mol.[24] The torsion angles about S_1–S_2 and S_1–$S_{2'}$ bonds each contribute 1.9 kcal/mol of strain, giving a total torsion strain of 19.6 kcal/mol for **6**-Ts(1). By contrast, only 2.8 kcal/mol of torsion strain[24] is present in **5**-Ts(1). Although contributions of bond angle strain may be somewhat greater for the latter, the considerably greater torsion strain in **6**-Ts(1) should raise the activation energy for ring inversion of the pentathiepin **6** significantly above that for the tetrathiepin **5**. As discussed in the previous section, this analysis is consistent with the relative energies calculated for **5**- and **6**-Ts(1)'s (Table IV) but does not support the result reported for ring inversion of the pentathiepin **10**.[17]

We may use the above information[8,24] to estimate the energy difference between the chair and twist-boat form of the unsymmetric 1,2,3,5-tetrathiepins **2** and **4**. Since relative to the chair conformer there is only one additional high energy S–S torsion angle of 45° in the twist-boat form, the latter should be about 3 kcal/mol less stable than the chair and should not be expected to be seen by NMR. This is indeed the case experimentally.

Two- and Three-Site Exchange Analysis. It is noted that the line-shape analysis for **2a**, **2b**, and **4a** involves two-site exchange (no intermediate observed) while analysis of the magnetization transfer data (**3b**) involves a three-site model. The latter, more elaborate energy profile is associated with rate constants for chair-chair interconversion which are greater by a factor of 2 than those associated with a direct two-site exchange even though the overall height of the energy barrier is the same in both cases. This difference arises because an exchange event interconverts half the twist-boat integrated intensity

(23) Based on CNDO/s and MMPI calculations, a counterintuitive structural assignment has been suggested for related cyclic polysulfur compounds: Guttenberger, H. G.; Bestmann, H. J.; Dickert, F. L.; Sorgensen, F. S.; Snyder, J. P. *J. Am. Chem. Soc.* **1981**, *103*, 159.

(24) Zeroka, D. L.; Dixon, D. A., to be published. Full PRDDO calculations of the torsional potential for H_2S_2 are scaled to the ab initio results.

with one methyl of the chair conformer and half with the other methyl. Thus, if the chair methyls are labeled as sites 1 and 2 and the coalesced twist-boat methyls as site 3, the site interconversions may be described by eq 1–3,

$$d[1]/dt = k_1[1] + 0.5k_{-1}[3] \quad (1)$$

$$d[2]/dt = -k_1[2] + 0.5k_{-1}[3] \quad (2)$$

$$d[3]/dt = +k_1[1] + k_1[2] - k_{-1}[3] \quad (3)$$

where k_1 is the rate constant for chair-to-twist boat and k_{-1} is the reverse. If this model is reduced to the two-site case, the steady state approximation in the intermediate 3 yields the appropriate substitution; e.g., for site 1

$$d[1]/dt = -k_1[1] + 0.5k_1([1] + [2])$$

$$= -0.5k_1[1] + 0.5k_1[2].$$

A factor of 2 in observed rate constants is therefore a simple consequence of the difference between a two-site and a three-site model. The significance of this difference is that it adds a factor of ln 2 to $\Delta S^{\ddagger}$ for **3b** compared to the remaining compounds.

Experimental Section

General Procedures. Melting points were taken with a Thomas-Hoover or a Buchi capillary melting point apparatus and are uncorrected. Infrared spectra were recorded on a Nicolet 7199 FT infrared spectrometer and are reported in reciprocal centimeters. Only strong bands are reported unless otherwise stated. Routine proton NMR were obtained at either 80 to 90 MHz with a Varian EM390 or an IBM NR80 FT instrument. NMR data are reported in parts per million (δ) downfield from tetramethylsilane in deuteriochloroform unless otherwise stated. Analyses were determined by Galbraith Laboratories, Inc., Knoxville, TN.

All magnetization transfer experiments were carried out on a Nicolet NT-360WB spectrometer operating at 360.905 MHz. Selective 180° inversion pulses between 18 and 26 ms were chosen by attenuating the output of the low-power transmitter.

The responses from all three sites for **3b** were analyzed by means of an iterative nonlinear least-squares computer program capable of handling multisite problems. The rate constants obtained from magnetization transfer or line-shape analysis were input to another weighted nonlinear least-squares program to provide the activation parameters. In the latter case, error estimates were obtained by assuming that the temperature was accurate to ±2 °C and that the rate constants were determined to ±10%. Temperature measurements made by replacing the sample tube with one containing a thermocouple showed a maximum deviation from the set point of 0.6 °C.

2,2-Dimethyl-7-phenyl-[1,3,4,5]tetrathiepino[6,7-*c*]pyrazole, 3,3-Dimethyl-7-phenyl-[1,2,4,5]tetrathiepino[6,7-*c*]pyrazole, and 4,4-Dimethyl-7-phenyl-[1,2,3,5]tetrathiepino[6,7-*c*]pyrazole. The synthesis of the tetrathiepins is exemplified by the preparation of **2a**, **3a**, and **4a**. To a slurry of **1a** (1.08 g, 3.57 mmol) in acetone (40 mL) and methylene chloride (10 mL) was added 23% aqueous ammonium sulfide (2.6 mL) dropwise over 30 min. The mixture was stirred 3 h at ambient temperature and became homogeneous. The solvent was removed at reduced pressure, and the residue was partitioned between water and methylene chloride. The phases were separated and the organic layer was washed with brine and dried over calcium sulfate. The crude product was flash chromatographed on silica (2 × 8 in., ether–hexane gradient) to give first 450 mg of a mixture enriched in **1a** and **2a** and then 550 mg of a mixture containing mostly **3a** and **4a**. Both mixtures were further purified by HPLC[25] to give 330 mg (33%) of recovered **1a**, 250 mg (22%) of **3a** as a white solid [mp 92–93 °C; NMR ($CDCl_3$) δ 8.1 (s, 1 H), 7.75–7.25 (m, 5 H), 2.2 (s, 3 H), 1.7 (s, 3 H); IR (KBr) 1596, 1505, 753; HRMS, *m/e* 311.9893], 240 mg (21%) of **2a** as a white solid [mp 140.5–143.5 °C; NMR ($CDCl_3$) δ 8.13 (s, 1 H), 7.9–7.25 (m, 5 H), 1.8 (s, 6 H); IR (KBr) 1599 (m), 1507, 1050 (m), 951, 756, 685; HRMS, *m/e* 311.9880], and 160 mg (14%) of **4a** as a white solid [mp 134.5–135.5 °C; NMR ($CDCl_3$) δ 8.1 (s, 1 H), 7.9–7.3 (m, 5 H), 1.85 (s, 6 H); IR (KBr) 1508, 1050 (m), 949, 760; HRMS, *m/e* 311.9886]. The compounds were further characterized by dynamic NMR, mass spectral fragmentation patterns, NOE, and X-ray analysis (**2a**) as described in the text.

2,2-Dimethyl-7-methyl-[1,3,4,5]tetrathiepino[6,7-*c*]pyrazole (2b): white solid (10%); mp 110–112.5 °C; NMR ($CDCl_3$) δ 7.5 (s, 1 H), 3.9 (s, 3 H), 1.72 (s, 6 H); IR (KBr) 1500, 1360, 1345, 1145, 1102, 725, 691, 645, 622. Anal. Calcd for $C_7H_{10}N_2S_4$: C, 33.58; H, 4.03. Found: C, 33.39; H, 4.09.

3,3-Dimethyl-7-methyl-[1,2,4,5]tetrathiepino[6,7-*c*]pyrazole (3b): white solid (15%); mp 106–108 °C; NMR ($CDCl_3$) δ 7.6 (s, 1 H), 3.88 (s, 3 H), 2.1 (s, 3 H), 1.65 (s, 3 H); IR (KBr) 3090, 1500, 1355, 1346, 1160, 1141, 1104, 725, 690, 620. Anal. Calcd for $C_7H_{10}N_2S_4$: C, 33.58; H, 4.03. Found: C, 33.70; H, 4.07.

Molecular Orbital Calculations. The ab initio molecular orbital calculations were done with the HONDO program package[26] on an IBM 3081 computer. The geometries were determined by using analytic gradient techniques.[27] The basis set for these calculations has the form (12s8p1d/9s5p1d/4s)/[5s3p1d/3s2p1d/2s] in the order S/C/H. The split valence basis set for S is from McLean and Chandler[28] and is augmented by a set of d orbital polarization functions with exponent of 0.60. The basis sets for C and H are from Dunning and Hay.[29] For reduction of the size of the basis set, polarization functions were not included on the hydrogens. Even so, the basis set for $C_3H_4S_4$ (**5**) has 133 contracted basis functions while that for $C_2H_2S_5$ (**6**) has 134 basis functions.

Our previous calculations[8] on H_2S_2 employed a full double ζ plus polarization basis set that agreed well with experiment. For calculations of larger molecular systems, we investigated the capability of the full double ζ basis set without polarization functions. With this basis set, the S–S bond distance in H_2S_2 is 2.250 Å as compared to our previous calculated value of 2.067 Å (2.055 Å experiment).[30] As a consequence the trans rotation barrier is 2.8 kcal/mol and the cis barrier is 5.6 kcal/mol as compared to our previously calculated SCF values of 5.8 and 8.3 kcal/mol. Thus the structures and conformational properties of S–S bonds cannot be studied without polarization functions on S.

Since the [5,3] basis set for S saves 4 variational orbitals over the [6,4] basis set for each sulfur, a substantial savings for polysulfur systems can be realized with the smaller basis set. We thus optimized H_2S_2 with the [5,3,1] basis set on S. The structure has r(S–S) = 2.065 Å, r(S–H) = 1.332 Å, θ(HSS) = 98.8°, and τ(HSSH) = 89.4°, which is in excellent agreement with our previously calculated structure that has r(S–S) = 2.067 Å, r(S–H) = 1.331 Å, θ(HSS) = 98.2°, and τ(HSSH) = 89.7°. Thus the split valence basis set with polarization functions can adequately describe the structure of S–S bonds.

The force fields were determined by using the rapid analytic second derivative methods[31] in GRADSCF[32] on a CRAY/1A. The MP-2 corrections[33] were obtained simultaneously. The calcula-

(25) HPLC, when required, used a Zorbax Sil column and a methylene chloride–hexane mixture for elution.

(26) (a) Dupuis, M.; Rys, J.; King, H. F. *J. Chem. Phys.* **1976**, *65*, 111. (b) King, H. F.; Dupuis, M.; Rys, J. *National Resource for Computer Chemistry Software Catalog*, Vol. 1, Program QHO2 (HONDO), 1980.

(27) (a) Komornicki, A.; Ishida, K.; Morokuma, K.; Ditchfield, R.; Conrad, M. *Chem. Phys. Lett.* **1977**, *45*, 595. McIver, J. A.; Komornicki, A., Jr. *Ibid.* **1971**, *10*, 303. (b) Pulay, P. In *Applications of Electronic Structure Theory*, Schaefer, H. F., Ed.; Plenum: New York, 1977; p 153.

(28) McLean, A. D.; Chandler, G. S. *J. Chem. Phys.* **1980**, *72*, 5639.

(29) Dunning, T. H., Jr.; Hay, P. J. In *Methods of Electronic Structure Theory*, Schaefer, H. F., III, Ed.; Plenum Press: New York, 1977; Chapter 1.

(30) Winnewisser, M.; Haase, J. *Z. Naturforsch.* **1958**, *231*, 56.

(31) King, H. F.; Komornicki, A. In *Geometrical Derivatives of Energy Surfaces and Molecular Properties*; Jorgenson, P., Simon, S. J., Eds.; *NATO ASI series C. Vol. 166*, D. Reidel: Dordrecht, 1986; p 207. King, H. F.; Komornicki, A. *J. Chem. Phys.* **1986**, *84*, 5645.

(32) GRADSCF is an ab initio gradient program system designed and written by A. Komornicki at Polyatomics Research.

(33) (a) Moller, C.; Plesset, M. S. *Phys. Rev.* **1934**, *46*, 618. (b) Pople, J. A.; Binkley, J. S.; Seeger, R. *Int. J. Quantum Chem. Symp.* **1976**, *10*, 1.

tions on the transition states were done as follows. Approximate structures for Ts(1) and Ts(2) were constructed and crudely optimized. The force fields at the new approximations to the geometries of Ts(1) and Ts(2) were then determined. This Cartesian Hessian was used as the initial guess for the Hessian for the σ optimization. The transition states were determined by minimizing the sum of the squares of the gradient vector (σ optimization) rather than minimizing the energy as is done in a geometry optimization.

Supplementary Material Available: Tables listing crystallographic details for **2a** and **2b**, final positional and thermal parameters, bond distances, bond angles, etc. (25 pages). Ordering information is given on any current masthead page.

Molecular Design of Crown Ethers. 4.[1,2] Syntheses and Selective Cation Binding of 16-Crown-5 and 19-Crown-6 Lariats

Mikio Ouchi,[3a] Yoshihisa Inoue,*[3a] Kazuhito Wada,[3a] Shin-ichi Iketani,[3a] Tadao Hakushi,[3a] and Edwin Weber*[3b]

Department of Applied Chemistry and Basic Research Laboratory, Himeji Institute of Technology, 2167 Shosha, Himeji, Hyogo 671-22, Japan, and Institut für Organische Chemie und Biochemie, Universität Bonn, D-5300 Bonn 1, West Germany

Received November 18, 1986

A number of new lariat 16-crown-5 and 19-crown-6 ethers possessing a variety of single or double side arm(s) were synthesized, and their cation-binding abilities were evaluated by solvent extraction technique. In general, the extractabilities of the 16-crown-5 lariats for most mono- and divalent cations increased gradually with extending oxyethylene side arm. However, sodium and silver ions, which are best size fitted to the crown cavity, showed peak extractability/selectivity at a specific length of the donating side arm. The complexation stoichiometry is 1:1 for all cations employed as confirmed by measurement of the extraction equilibrium constants for the single-armed 16-crown-5 (**3p**). The tetrasubstituted pivot carbon is shown to be a requirement for lariat 16-crown-5 to effect extra side-arm ligation, although the second side arm of lariat ether **3e** seems ineffective in extractability enhancement with reference to the single-armed analogue **3p**. By contrast, the corresponding 19-crown-6 lariats with potential donor side arms at an appropriate position did not show any enhancement in extractability for most cations, which may be attributed to its flexible framework.

Lariat ethers[4] have been designed to enhance the cation-binding ability of common crown ethers by introducing a side arm carrying extra donor group(s) and also to partly mimic the dynamic complexation process shown by natural macrocyclic ligands. As has been demonstrated by several research groups,[2,4-6] some carbon- and nitrogen-pivot lariat ethers indeed exhibit higher cation-binding abilities than the parent crown ethers probably through further ligation of side-arm donors. From the standpoint of synthetic feasibility, the usual lariat ethers are predominantly based on common 3*m*-crown-*m* ethers or their aza analogues. On the other hand, they may not necessarily be the best choice in respect of cation selectivity.

We have recently reported that less symmetrical (3*m*+*n*)-crown-*m* ethers show lower extractabilities in general but exhibit drastically different and, in some cases, higher selectivities for specific cations.[7] 16-Crown-5, in particular, shows much higher cation selectivity for Na^+ and Ag^+ than any other crown-5. This behavior prompted us to use the 16-crown-5 framework for the design of lariat ethers with enhanced cation-binding ability and selectivity. We now report the syntheses of a variety of lariat 16-crown-5 and, for comparison purpose, 19-crown-6 ethers with different single and double side arms. They are composed of long alkyl and/or oxyethylene chains attached through a carbon pivot. The cation-binding ability of the new lariat ethers evaluated from solvent extraction of aqueous alkali, alkaline-earth, and some heavy-metal picrates is discussed (Chart I).

Results

Syntheses. Double-armed 16-crown-5 ethers **3e–3j** were synthesized in 60–78% yields by reaction of the corresponding oligoethylene glycol monomethyl ether tosylates **6a–6f** with 15,15-bis(hydroxymethyl)-16-crown-5 (**3d**)[7a,10] in the presence of NaOH (or NaH) as a base in THF. The acyclic ligand **5c** was obtained from 2,2-dimethyl-1,3-propanediol and **6d** in 79% yield.

The 16-crown-5 derivative **3m** with a single oxyethylene chain was synthesized analogously from (hydroxymethyl)-16-crown-5 (**3l**) and **6a**. **3l** was prepared by hydroboration of 15-methylene-16-crown-5 (**3k**)[8] in 83% yield.

For the single-armed lariat ethers with a methyl group at the pivot, i.e. **3p**, **3q**, **4f**, and **4g**, two different routes were applied. The first reaction path involves the synthesis of **8b** by reaction of 5-(hydroxymethyl)-2,2,5-trimethyl-1,3-dioxane (**8a**)[2b] with **6a**. **8a** was obtained from 2-(hydroxymethyl)-2-methyl-1,3-propanediol by treatment with

(1) Part 3: Inoue, Y.; Ouchi, M.; Hakushi, T. *Bull. Chem. Soc. Jpn.* **1985**, *58*, 525.
(2) Preliminary reports: (a) Ouchi, M.; Inoue, Y.; Wada, K.; Hakushi, T. *Chem. Lett.* **1984**, 1137. (b) Weber, E. *Liebigs Ann. Chem.* **1983**, 770. (c) Offermann, W.; Weber, E. *Chem. Ber.* **1984**, *117*, 234.
(3) (a) Himeji Institute of Technology. (b) Universität Bonn.
(4) (a) Dishong, D. M.; Diamond, C. J.; Cinaman, M. I.; Gokel, G. W. *J. Am. Chem. Soc.* **1983**, *105*, 586. (b) Schultz, R. A.; White, B. D.; Arnold, K. A.; Gokel, G. W. *Ibid.* **1985**, *107*, 6659.
(5) (a) Ikeda, I.; Emura, H.; Okahara, M. *Bull. Chem. Soc. Jpn.* **1985**, *57*, 1612. (b) Nakatsuji, Y.; Nakamura, T.; Okahara, M.; Dishong, D. M.; Gokel, G. W. *J. Org. Chem.* **1983**, *48*, 1237. (c) Nakatsuji, Y.; Nakamura, T.; Okahara, M. *Chem. Lett.* **1982**, 1207.
(6) Tsukube, H.; Takagi, K.; Higashiyama, T.; Hayama, N. *J. Chem. Soc., Perkin Trans. 1* **1986**, 1033.
(7) (a) Ouchi, M.; Inoue, Y.; Sakamoto, H.; Yamahira, A.; Yoshinaga, M.; Hakushi, T. *J. Org. Chem.* **1983**, *48*, 3168. (b) Ouchi, M.; Inoue, Y.; Kanzaki, T.; Hakushi, T. *Ibid.* **1984**, *49*, 1408. (c) Inoue, Y.; Ouchi, M.; Hakushi, T. *Bull. Chem. Soc. Jpn.* **1985**, *58*, 525. The K_{ex} values for divalent cations were reported erroneously and should read as reported here.
(8) Tomoi, M.; Abe, O.; Ikeda, M.; Kihara, K.; Kakiuchi, H. *Tetrahedron Lett.* **1978**, 3031.
(9) Blicke, F. F.; Zienty, M. F. *J. Am. Chem. Soc.* **1941**, *63*, 2779.
(10) (a) Weber, E. *Angew. Chem.* **1979**, *91*, 230; *Angew. Chem., Int. Ed. Engl.* **1979**, *18*, 219. (b) Weber, E. *J. Org. Chem.* **1982**, *47*, 3478.

0022-3263/87/1952-2420$01.50/0